Granular Impact Cratering by Liquid Drops: An Analogy to Asteroid Strikes

Runchen Zhao, Professor Xiang Cheng

Department of Chemical Engineering and Materials Science, University of Minnesota

Introduction

When a granular material is impacted by a sphere, its surface deforms like a liquid yet it preserves a circular crater like a solid. We investigate liquid-drop impact dynamics on granular surface and monitor the morphology of resulting impact craters. Surprisingly, we find that despite the enormous energy and length difference, granular impact cratering by liquid drops follows the same energy scaling and reproduces the same crater morphology as that of asteroid impact crater. We integrate the physical insight from planetary sciences, the liquid marble model from fluid mechanics, and the concept of jamming transition from granular physics into a simple theoretical framework that quantitatively describes all of the main features of liquid-drop imprints in granular media.

Methods

We release a stationary water drop of diameter D=1.4-4.6 mm from a height h. The drop falls vertically in air onto a granular bed comprising d_{sand} = 45-250 µm glass beads with volume fraction φ =0:60. We vary h from 1.8 mm up to 12 m. A Photron SA-X2 camera was used for high-speed imaging of drop impact dynamics. The morphology of impact craters was measured using a high precision laser profilometer. The camera and the profilometer were further combined to monitor the depth of crater during impacts. We also performed one set of experiments at one-tenth of the atmospheric pressure to test possible effects of ambient air on the dynamics of liquid-drop impact cratering.

Results

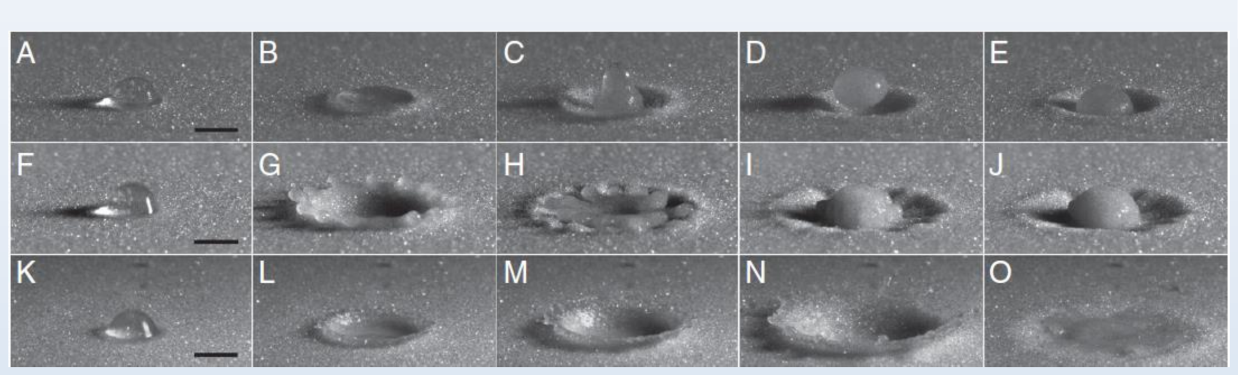

Fig. 1. Impact of a water drop on a granular surface. Snapshots from high-speed movies showing the impact of a 3.1 mm water drop with E =7.8 × 10−6 J (A–E), E =6.0 × 10−5 J (F–J), and 2.3 × 10−4 J (K–O)

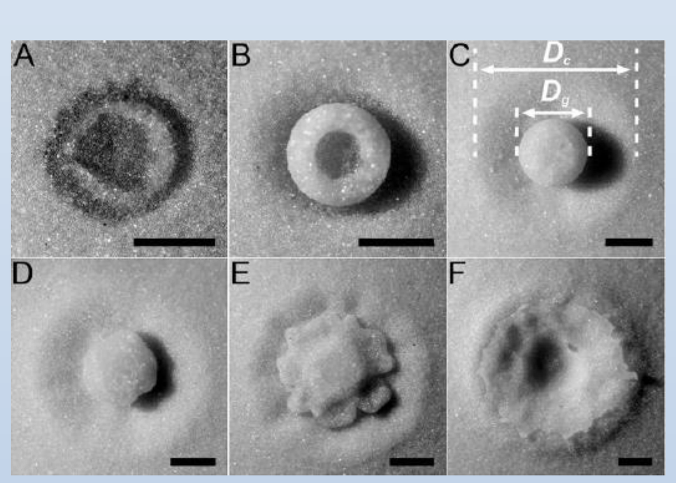

Fig. 2. Morphology of liquid-drop impact craters. Impact craters from the strike of a 3.1-mm water drop with E =9:7 × 10−7 J (A), 6:5 × 10−6 J (B), 3:2 × 10−5 J (C), 6:0 × 10−5 J (D), 8:2 × 10−5 J (E), and 3:0 × 10−4 J (F). Scale bars: 3.0 mm. D_c and D_g are defined in C.

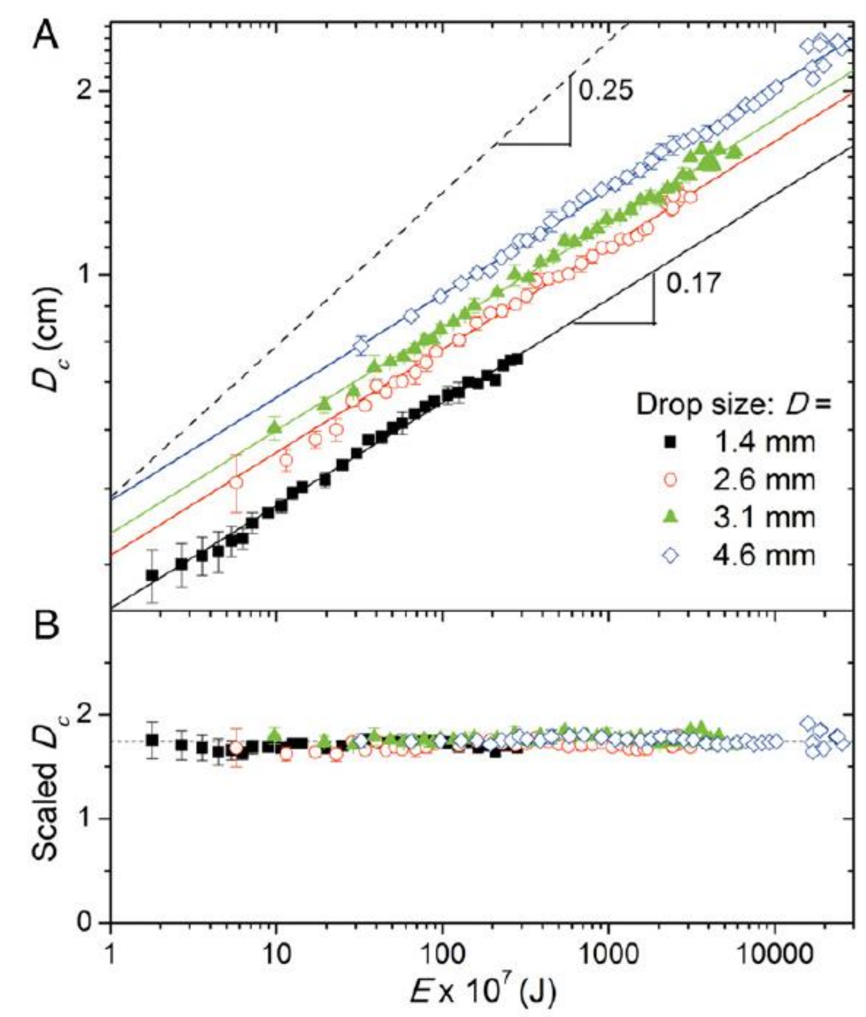

Fig. 3. Scaling of liquid-drop impact craters. (A) D_c versus E for different drop sizes. (B) Scaled Dc following the S-H scaling rule.

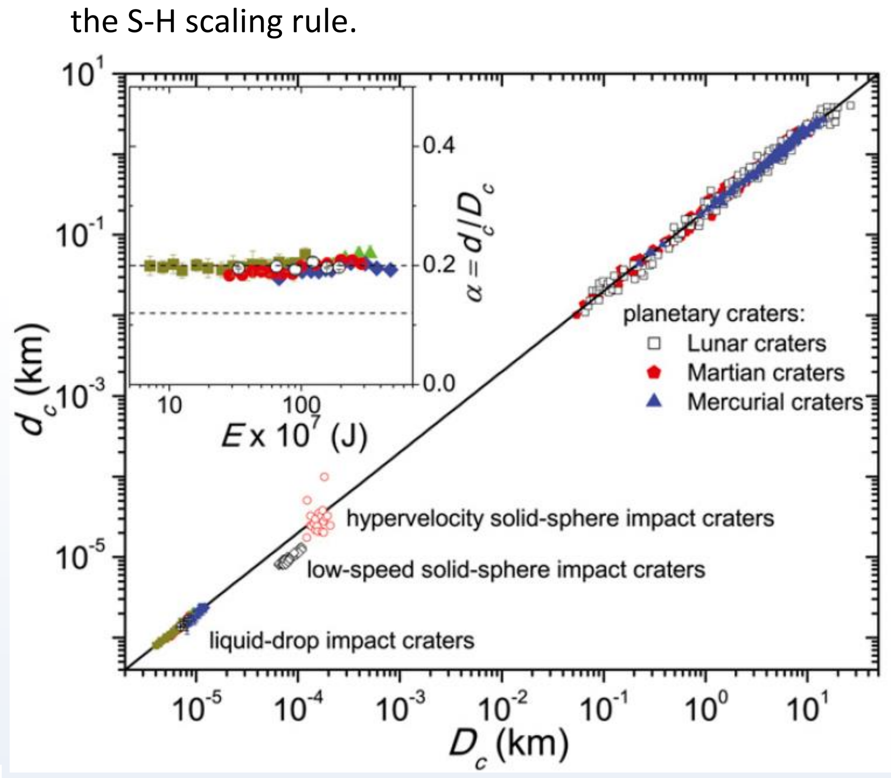

Fig. 4. Aspect ratio of liquid-drop impact craters. D_c versus D_c for four different impact cratering processes. (Insets) d_c/D_c of liquid-drop impact craters. The upper and lower dashed lines indicate the aspect ratio of planetary impact craters (0.20) and low speed solid-sphere impact craters (0.12), respectively.

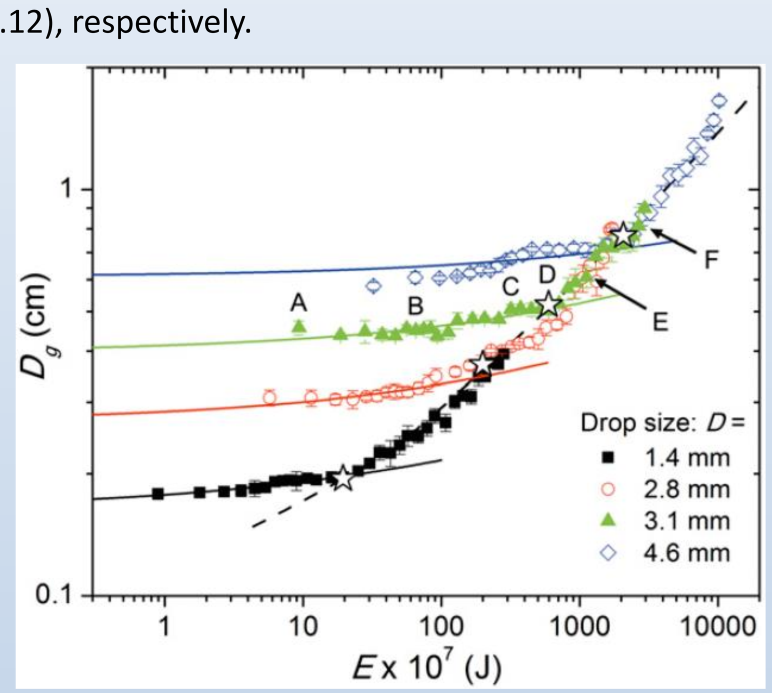

Fig. 5. Morphology of granular residues. Crater morphologies shown in Fig. 2 A–F are indicated. Stars mark the transition impact energy E* between the low- and high-E regime for each drop size. Solid lines are from the liquid marble model. The dashed line is $D_g(E^*)$ calculated by combining the liquid marble model with the jamming criterion.

Surprisingly, the 0.17 scaling is quantitatively similar to the Schmidt–Holsapple (S-H) scaling from hypervelocity impact cratering associated with asteroid strikes.

$$D_c \sim g^{-0.17} D^{0.83} U^{0.34} \sim (\rho g)^{-0.17} D^{0.32} E^{0.17}$$

1. Liquid Impact Model for Crater Diameter:

Impact Energy Conversion

$$E_{eject} = f E_{impact}$$

$$f = \frac{\pi D^2}{\pi D_c^2}$$

Contribution of Eject Energy

$$E_{\rm eject} \approx \rho_{\rm sand} V_{\rm crater}\, g\, d_{\rm depth}$$

* w/ Spherical Cap Approximation

$$V_{\rm crater} = \frac{\pi\alpha^2}{6}(3-2\alpha)D_{\rm crater}^3 \qquad d_{\rm depth} = \alpha D_{\rm crater}$$

$$D_{\rm crater} \approx \left(\frac{\pi}{6}\alpha^3(3-2\alpha)\frac{\rho_{\rm sand}}{\rho_{\rm drop}}\right)^{-1/6} \cdot [(\rho_{\rm drop} g)^{-1/6} \cdot D_{\rm drop}^{1/3} \cdot E_{\rm impact}^{1/6}] \qquad \text{Prefactor=1.74}$$

2. Liquid Marble Theory and Imbibition Model for Granular Residue:

Low Energy Regime

$$N \approx \frac{\pi(D_{\rm crater}/2)^2}{\pi(d_{\rm sand}/2)^2} = \left(\frac{D_{\rm crater}}{d_{\rm sand}}\right)^2 \qquad V_{\rm marble} = \frac{\pi}{6}D_{\rm drop}^3 + N\frac{\pi}{6}d_{\rm sand}^3 = \frac{\pi}{6}D_{\rm drop}^3 + \frac{\pi}{6}D_{\rm crater}^2 d_{\rm sand}$$

Number of particles adsorbed at surface

Liquid Marble Volume

Spherical Shape Maintenance Criteria , $\kappa^{1} = (\gamma/\rho g)^{1/2}$ Capillary length

$$\begin{cases} D_{\rm marble} \ll \kappa^{-1} \longrightarrow \text{Spherical} \longrightarrow D_{\rm marble} = (6V_{\rm marble}/\pi)^{1/3} \\ D_{\rm marble} \gg \kappa^{-1} \longrightarrow \text{Puddle} \longrightarrow D_{\rm marble} \approx (3V_{\rm marble}/\pi\kappa^{-1})^{1/2} \end{cases}$$

$$D_{\rm granular} = \begin{cases} C_1 \cdot (D_{\rm drop}{}^3 + 3.02(\rho_{\rm drop} g)^{-0.34} D_{\rm drop}{}^{0.64} E_{\rm impact}{}^{0.34} d_{\rm sand})^{1/3} & \text{for} \quad D_{\rm marble} < \kappa^{-1} \\ C_2 \cdot [(D_{\rm drop}{}^3 + 3.02(\rho_{\rm drop} g)^{-0.34} D_{\rm drop}{}^{0.64} E_{\rm impact}{}^{0.34} d_{\rm sand})/2\kappa^{-1}]^{1/2} & \text{for} \quad D_{\rm marble} > \kappa^{-1}. \end{cases}$$

High Energy Regime

Washburn-Lucas Equation for Imbibition

$$V_{imb} = \frac{\pi}{2}\left(\frac{t}{\mu}\right)^{\frac{1}{2}} \sum \left(P_E + \frac{2\gamma}{a}cos\theta\right)^{\frac{1}{2}} a^3$$

Modify parameters and yield:

$$V_{imb} = 0.058A(\mu^2\gamma)^{\frac{1}{4}}\rho^{\frac{1}{4}} d_{sand} D^{\frac{5}{4}} E^{\frac{1}{2}}$$

Imbibition-Jamming Model:

$$\frac{V_{sand}}{V_m - V_{imb}} = \frac{\frac{\pi d_{sand} D_c^2}{6}}{\frac{\pi D^3}{6} + \frac{\pi d_{sand} D_c^2}{6} - V_{imb}} = \varphi_c$$

Numerically solve it to give E vs. D_g. Plotted in Figure 5 on the left.

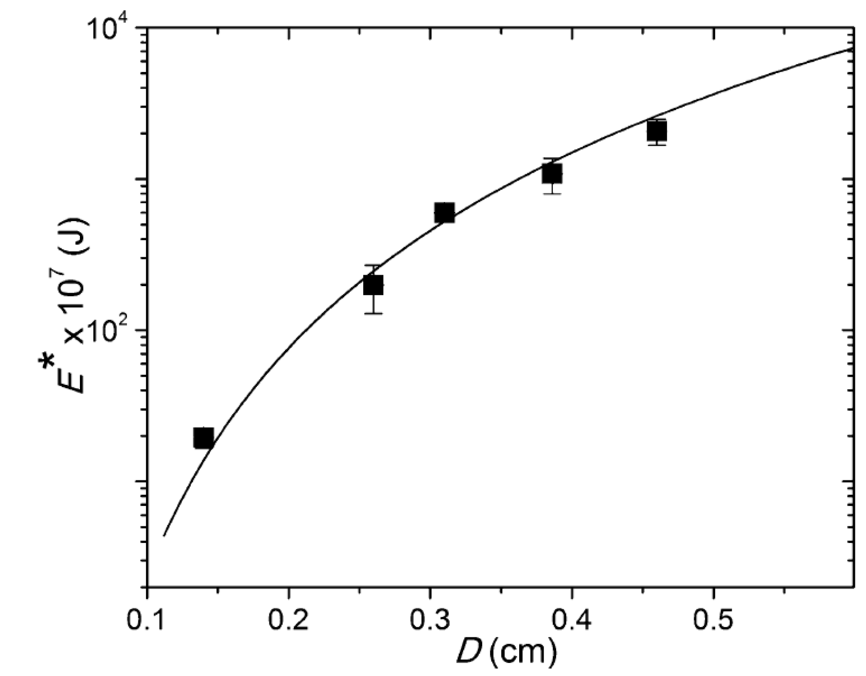

Fig. 6. Transition energy E* versus drop size D. Solid line is based on the jamming criterion.

Conclusion

When a liquid drop impacts on a granular surface, the impact energy is converted into the surface energy of the deformed drop, the internal energy of liquid and particles, and the kinetic energy of the spreading lamella and ejected particles. The process is notoriously complicated, involving high Reynolds hydrodynamics, shock compression in the impinging drop, fast granular flows, and capillary interactions between fluid and granular particles. Given the complexity, it is surprising that the simple model presented here can quantitatively capture the morphology of liquid-drop impact craters over a large range of impact energy.

Moreover, our study reveals a quantitative similarity between raindrop impact cratering and asteroid impact cratering in terms of both the energy scaling and the aspect ratio of their impact craters. Compared with extensively studied low-speed solid sphere impact cratering, liquid-drop impact cratering provides a better analogy to high-energy asteroid impact cratering. Apparently, one should be very cautious when drawing a close link between the two processes. Nevertheless, the remarkable similarity between the two processes indicates that they may share common mechanisms that are worth further investigation.

Selected Reference

1. Zhao, R; Zhang, Q; Tjugito, H; Cheng ,X (2015). Granular impact cratering by liquid drops: Understanding raindrop imprints through an analogy of asteroid strikes. *Proc. Natl. Acad. Sci.* **112**,342-347.
2. Katsuragi, H (2010). Morphology Scaling of Drop Impact onto a Granular Layer. *Phys. Rev. Lett.* **104**, 218001
3. Aussillous, P; Quéré, Q (2001). Liquid Marbles. *Nature* **411**, 924

Acknowledgement

This work is funded by the University of Minnesota Undergraduate Research Opportunity Program (UROP)